Development of New Hepaticoenteric Collateral Pathways after Hepatic Arterial Skeletonization in Preparation for Yttrium-90 Radioembolization

Mohamed H.K. Abdelmaksoud, MD, MS, Gloria L. Hwang, MD, John D. Louie, MD, Nishita Kothary, MD, Lawrence V. Hofmann, MD, William T. Kuo, MD, David M. Hovsepian, MD, and Daniel Y. Sze, MD, PhD

PURPOSE: Development of new hepaticoenteric anastomotic vessels may occur after endovascular skeletonization of the hepatic artery. Left untreated, they can serve as pathways for nontarget radioembolization. The authors reviewed the incidence, anatomy, management, and significance of collateral vessel formation in patients undergoing radioembolization.

MATERIALS AND METHODS: One hundred thirty-eight treatments performed on 122 patients were reviewed. Each patient underwent a preparatory digital subtraction angiogram (DSA) and embolization of all hepaticoenteric vessels in preparation for yttrium-90 (^{90}Y) administration. Successful skeletonization was verified by C-arm computed tomography (CACT) and technetium-99m macroaggregated albumin (^{99m}TcMAA) scintigraphy. During the subsequent treatment session, DSA and CACT were repeated before administration of ^{90}Y, and the detection of extrahepatic perfusion prompted additional embolization.

RESULTS: Forty-two patients (34.4%) undergoing 43 treatments (31.2%) required adjunctive embolization of hepaticoenteric vessels immediately before ^{90}Y administration. Previous scintigraphy findings showed extrahepatic perfusion in only three cases (7.1%). Vessels were identified by DSA in 54.1%, by CACT in 4.9%, or required both in 41.0%. The time interval between angiograms did not correlate with risk of requiring reembolization ($P = .297$). A total of 19.7% of vessels were new collateral vessels not visible during the initial angiography. Despite reembolization, three patients (7.1%) had gastric or duodenal ulceration, compared with 1.3% who never had visible collateral vessels, all of whom underwent whole-liver treatment with resin microspheres ($P = .038$).

CONCLUSIONS: Development of collateral hepaticoenteric anastomoses occurs after endovascular skeletonization of the hepatic artery. Identified vessels may be managed by adjunctive embolization, but patients appear to remain at increased risk for gastrointestinal complications.

PRIMARY and metastatic hepatic malignancies are a major source of morbidity and mortality worldwide and continue to be difficult to manage. Because so few patients are eligible for resection or transplant, and systemic medical therapies have limited response rates and durations, image-guided locoregional therapies have assumed a substantial role in the treatment of these patients. Selective intraarterial radiotherapy with beta–particle-emitting microspheres (radioembolization) helps with the direct delivery of high-dose radiation to hepatic tumors by exploiting the dual vasculature of the liver to target tumors that are supplied primarily by hepatic arterial blood [1,2]. Microspheres of ~30 μm diameter loaded with the beta-emitter yttrium-90 (^{90}Y) are administered intraarterially and lodge preferentially in tumor vasculature, thereby confining the tumoricidal dose to the immediate proximity of the tumors with relative sparing of the portal venous-supplied normal hepatic parenchyma.

Earliest investigations into radioembolization starting in the 1960s were limited by gastrointestinal ulceration and hemorrhage, leading to the recognition of nontarget radioembolization through hepaticoenteric anastomoses [3,4]. Although some resultant ulcers responded to medical treatment, some required surgical intervention, and some were fatal [5,6]. To prevent these complications, meticulous pretreatment angiography and skeletonization of the hepatic artery

Table 1
Patient Demographics

	n	%
Age, y		
≤ 30	4	3.3
31–40	6	4.9
41–50	12	9.8
51–60	32	26.2
61–70	43	35.2
71–80	22	18.0
> 80	3	2.5
Sex		
Male	75	61.5
Female	47	38.5
Diagnosis		
Primary	27	22.1
Metastatic	95	77.9
Total patients	122	
Total treatments	136	
Mean treatments per patient	1.1	

Table 2
Tumor Cell Types Treated

	n	%
Primary	27	22.1
Hepatocellular carcinoma	21	17.2
Cholangiocarcinoma	5	4.1
Cholangiohepatoma	1	0.8
Metastatic	95	77.9
Colorectal	44	36.1
Neuroendocrine, including carcinoid	14	11.5
Other gastrointestinal, including gastric, esophageal, pancreatic, gallbladder	8	6.6
Renal cell	5	4.1
Melanoma	5	4.1
Adenocarcinoma of unknown primary	4	3.3
Lung, non–small cell	3	2.5
Sarcoma	3	2.5
Ovarian (epithelial)	2	1.6
Thymic	2	1.6
Breast	2	1.6
Hemangiopericytoma	1	0.8
Ovarian (granulosa cell)	1	0.8
Lymphoma	1	0.8
Total	122	

Table 3
Details of Radioembolization Procedures

	Patients (n)	Patients (%)	Procedures (n)	Procedures (%)
Type of radioembolization microsphere used				
SIR-Spheres	109	89.3	119	86.2
TheraSphere	13	10.7	19	13.8
Territory of liver treatment				
Whole liver	84	68.9	100	72.5
Proper hepatic artery single administration	61	50	64	46.4
Two lobar administrations during single procedure	10	8.2	10	7.2
Two lobar administrations sequentially at different procedure sessions	13	10.7	26	18.8
Right lobe only	31	25.4	31	22.5
Left lobe only	3	2.5	3	2.2
Right lobe and segment IV	3	2.5	3	2.2
Segment IV only	1	0.8	1	0.7

have become essential preludes to radioembolization therapy (2,7). The gastroduodenal artery (GDA) and right gastric artery (RGA) are routinely amenable to prophylactic coil embolization, but numerous smaller vessels originating from the hepatic vasculature may also require embolization, which can be technically challenging (8,9). An intraarterial injection of technetium-99m–labeled macroaggregated albumin (^{99m}Tc-MAA) is used to quantitate shunting into the pulmonary vasculature but is also useful for detection of extrahepatic perfusion. The spatial resolution of scintigraphy is limited, however, especially for the resolution of neighboring organs such as the stomach, duodenum, and pancreas, which are in direct contact with the liver (10).

On the day of ^{90}Y administration, hepatic angiography is repeated to confirm catheter position and to verify the durability of the skeletonization of the hepatic artery. Both digital subtraction angiography (DSA) and C-arm computed tomography (CACT) scans may reveal persistent or new extrahepatic perfusion, either from incomplete occlusion of previously treated vessels or from appearance of new collateral vessels (11). We reviewed the incidence, anatomic patterns, endovascular management, and clinical significance of finding residual or new hepaticoenteric anasto-moses at the time of administration of radioembolic microspheres.

MATERIALS AND METHODS

Study Population

From June 2004 to May 2009, 122 consecutive patients with hepatic malignancy underwent 138 radioembolization administrations (SIR-Spheres, Sirtex Medical Inc., Wilmington, Mas-sachusetts, or TheraSphere, MDS Nordion, Ottawa, Canada) and were included in this retrospective study. These include three patients who underwent whole-liver retreatment a year or more after initial treatment and repeated the entire preparatory process before their second treatments. One patient was excluded from the analysis because she underwent the preparatory angiogram and right lobe treatment session at another insti-

Table 4
Hepaticoenteric Anastomotic Arteries Embolized during Preparatory Angiography

	n	%
Gastroduodenal artery	99	81.1
Right gastric artery	81	66.4
Pancreaticoduodenal artery	22	18.0
Supraduodenal artery	21	17.2
Dorsal pancreatic artery	17	13.9
LGA (including accessory LGA)	4	3.3
Falciform artery	3	2.5
Total	247	
Mean arteries per patient	2.0	

Table 5
Hepaticoenteric Anastomotic Arteries Requiring Adjunctive Embolization Immediately before [90]Y Administration

	n	%
Total arteries needing adjunctive embolization	61	
Previously embolized arteries needing reembolization	14	23.0
New arteries needing embolization	47	77.0
Number of arteries needing embolization per patient		
One artery	28	65.1
Two arteries	12	27.9
Three arteries	3	7.0
Specific arteries needing embolization or reembolization		
Right gastric artery (including accessory RGA)	20	32.8
Supraduodenal artery	17	27.9
Gastroduodenal artery	6	9.8
Left gastric artery (including accessory LGA)	5	8.2
Cystic and ductal arteries	4	6.6
Falciform artery	4	6.6
Pancreaticoduodenal artery	3	4.9
Dorsal pancreatic artery	2	3.3
Vascular territory supplied by hepaticoenteric arteries needing embolization or reembolization ($N = 61$):		
Stomach	23	37.7
Duodenum	22	36.1
Biliary system	4	6.6
Pancreas	4	6.6
Thoracic and abdominal wall	4	6.6
Stomach and duodenum	3	4.9
Stomach and pancreas	1	1.6
Arteries needing reembolization but not successfully catheterized ($N = 7$):		
Supraduodenal artery	3	42.9
Right gastric artery (including accessory RGA)	3	42.9
Falciform artery	1	14.3

tution before being evaluated by us (**Table 1**). All data were handled in compliance with the Health Insurance Portability and Accountability Act. The institutional review board of our institution waived the requirement for obtaining patient consent for this retrospective study.

The population comprised 75 men (61.5%) and 47 women (38.5%) whose ages ranged from 20 to 84 years (mean, 60.1; median, 61; **Table 1**). Twenty-seven (22.1%) had primary hepatic malignancy (hepatocellular carcinoma, cholangiocarcinoma, and cholangiohepatoma), and 95 (77.9%) had metastatic disease, including adenocarcinoma of unknown origin. The sites of primary malignancy are listed in **Table 2**.

One hundred nine patients (89.3%) underwent radioembolization with SIR-Spheres, and 13 patients (10.7%) underwent treatment with TheraSphere (**Table 3**). The majority of patients who underwent SIR-Spheres radioembolization had diffuse bilobar metastatic disease and thus received whole-liver treatment. Single-session whole-liver treatment was performed for 74 treatments (53.6%) on 71 patients to limit the potential for tumor progression in an untreated lobe and to minimize issues involving health insurance companies refusing to reimburse multiple administrations. Patients with compromised liver function or performance status requiring whole-liver treatment underwent staged sequential lobar treatments. All patients undergoing TheraSphere radioembolization underwent lobar or

segmental treatment because most were treated for single lesions.

Angiography and Embolization Procedure

All patients underwent a preparatory hepatic angiogram to map out hepatic vasculature, to identify replaced or accessory hepatic arteries, to embolize visible hepaticoenteric anastomoses, and to inject a tracer dose of ^{99m}TcMAA for scintigraphy. Details about imaging protocols were previously reported (11). Briefly, a ceiling-mounted C-arm system (Axiom Artis dTA; Siemens, Erlangen, Germany) was used for both DSA and CACT, and data were processed on a separate workstation (Syngo-X, Siemens). Multiplanar reconstructions of CACT were used predominantly for identification of extrahepatic parenchymal enhancement, and DSA and volume-rendered CACT images were used primarily for identification of individual vessels.

All branch arteries leading to nonhepatic vascular beds that were in close proximity to or within the anticipated distribution of the site of injection were selected and embolized to stasis. The largest arteries (> 5 mm luminal diameter, measured by electronic calipers) were selected with a 5-F diagnostic catheter (Beacon Tip; Cook, Inc, Bloomington, Indiana) or introducer guide (Vista Brite-tip IG; Cordis, Inc, Warren, New Jersey) and embolized with 0.035-inch coils (Tornado and/or Nester; Cook, Inc) or a vascular plug in three patients in whom access was not tortuous (Amplatzer or Amplatzer 2; AGA Medical, Inc, Plymouth, Minnesota). Mid-sized arteries (3–5 mm diameter) were selected using 5-F diagnostic catheters and embolized with 0.035-inch coils. Smaller arteries (1–4 mm diameter) were selected using microcatheters (ProGreat 2.4; Terumo Medical, Som-
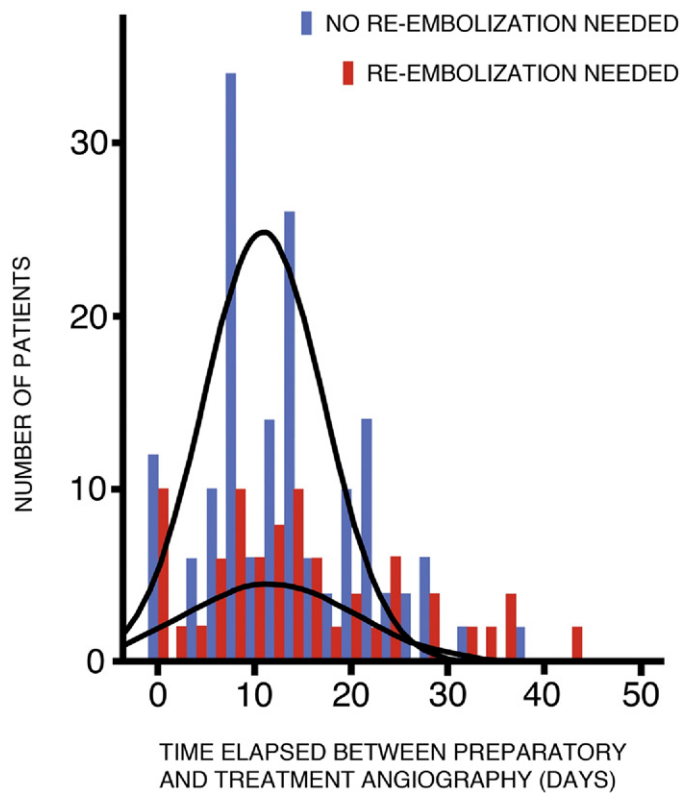
Figure 1. Differences in distributions of time intervals between the preparatory angiogram and the treatment administration in those requiring and those not requiring adjunctive embolization were not statistically significant ($P = .297$). Longest intervals represent patients who suffered complications of the preparatory angiogram (contrast medium-induced nephropathy, arterial dissection), had health insurance issues, or requested delays.

Table 7
Etiology of Appearance of Arteries Requiring Adjunctive Embolization

	n	%
Vessel was not apparent on preparatory angiography	12	19.7
Interval hypertrophy of vessel	9	14.8
Reversal of flow of vessel	3	4.9
Vessel was apparent on preparatory angiography	49	80.3
Attempt to catheterize was unsuccessful	19	31.1
Vessel too small to catheterize, embolization not attempted	10	16.4
Coil embolized but still patent:		
Persistent flow through coils	10	16.4
Proximal branch not occluded	4	6.6
Physician error, misinterpretation of images	6	9.8

Table 6
Detection of Arteries Requiring Adjunctive Embolization

	n	%
Imaging modality required to identify artery		
DSA	33	54.1
CACT only	3	4.9
Both DSA and CACT	25	41.0
Diameter of previously embolized artery requiring reembolization		
0–2 mm	5	35.7
2.1–4 mm	3	21.4
> 4 mm	6	42.9
Diameter of new artery requiring embolization		
0–2 mm	36	76.6
2.1–4 mm	10	21.3
> 4 mm	1	2.1

Note.—CACT = C-arm computed tomography.

erset, New Jersey, or J-tipped Prowler Plus; Cordis Neurovascular, Inc, Miami Lakes, Florida) and embolized with 0.018-inch coils (VortX; Target/Boston Scientific, Inc, Natick, Massachusetts; Tornado, MicroNester; Cook, and/or Azur; Terumo). The smallest arteries (< 1 mm diameter) required smaller-caliber microcatheters (Prowler 14 or Prowler 10; Cordis Neurovascular) and detachable coils (Microcoil; Micrus Endovascular, San Jose, California). All visible hepaticoenteric communications were embo-lized, whether the patient was to undergo glass or resin microsphere treatment, and whether whole-liver, lobar, or segmental treatment was planned.

After coil embolization of visible hepaticoenteric anastomoses, completion DSA was performed to determine completeness of skeletonization, and any incompletely treated vessels or any immediately appearing collateral vessels were selected and embolized. Contrast-enhanced CACT with injection of contrast medium into the common hepatic artery was also performed to look for any extrahepatic tissue enhancement suggesting persistent hepaticoenteric communication, and, if found, additional selective DSA and embolization were performed. Parasitized extrahepatic arteries were also embolized, but these anastomoses typically result in incomplete hepatic treatment rather than extrahepatic nontarget radioembolization and were thus excluded from these statistical analyses. Finally, approximately 1 mCi of ^{99m}TcMAA was injected at the planned administration site in each patient. A dose lower than the standard 4–5 mCi was used to allow for
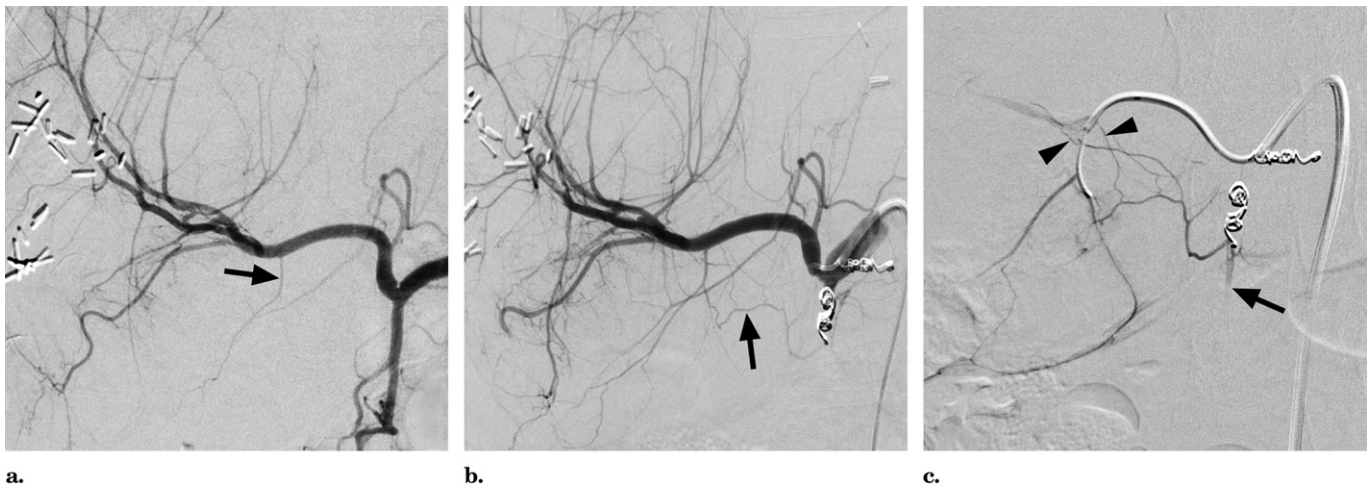
Figure 2. A 50-year-old woman with metastatic colon adenocarcinoma underwent radioembolization for progressive bilobar hepatic metastases. She had undergone previous resection of the primary tumor, partial right hepatectomy, intraoperative radiofrequency ablation, percutaneous radiofrequency ablation, and numerous systemic chemotherapy regimens including FOLFOX, irinotecan, capecitabine, bevacizumab, and cetuximab. **(a)** The initial hepatic arteriogram showed a small and unbranched cystic artery (arrow). The GDA and RGA were selected and coil embolized. **(b)** Just before radioembolic microsphere administration 28 days later, repeat hepatic arteriogram showed interval hypertrophy of the cystic artery and appearance of branches coursing toward the duodenum (arrow). **(c)** Selection of the medial branch of the cystic artery confirmed supply to the distal GDA (arrow) via a hilar and ductal artery network, which also included two additional supraduodenal branches contiguous with the right hepatic artery with hepatopetal flow (arrowheads). This arcade no longer opacified on hepatic arteriography after coil embolization of the medial branch of the cystic artery. She underwent single-session whole-liver treatment with administration into the proper hepatic artery without gastrointestinal complications.

fusion ⁹⁹ᵐTcMAA/⁹⁹ᵐTc-sulfur colloid imaging (12). Patients then underwent planar and single photon emission computed tomography (SPECT) imaging to calculate lung shunt fraction and to assess for extrahepatic perfusion. The arteries embolized during the preparatory angiogram are listed in Table 4.

When patients returned for the radioembolic microsphere administration, all underwent repeat DSA and contrast-enhanced CACT to reevaluate the completeness and durability of skeletonization of the hepatic artery (11). Any identified extrahepatic perfusion or parasitized vessel was subjected to further angiography and coil embolization when possible before administration of the radioembolic microspheres. If an identified hepaticoenteric arterial anastomosis could not be successfully catheterized and embolized, then the microcatheter was positioned distal to the vessel origin, and extra caution was exercised during delivery of the radioembolic material to prevent reflux. If the vessel origin was near a bifurcation, the dose was split, and a proportional fraction was delivered into each branch.

Image Analysis and Data Collection

DSA and CACT images from the preparatory angiogram and from the treatment session were reviewed retrospectively, and the following data were collected: treated vessels requiring additional embolization, collateral vessels that appeared de novo or hypertrophied and required embolization, the anatomic origins and the vascular territories supplied by these vessels, the number and the diameter of each vessel, whether the collateral vessel was seen on the preparatory angiogram prospectively or retrospectively, which imaging modality was needed to identify the vessel (DSA or CACT or both), technical success of reembolization attempt, whether the ⁹⁹ᵐTcMAA scintigraphy identified extrahepatic perfusion, and the time interval between the preparatory angiogram and the treatment session.

A commercial software package (SPSS v. 17.0.0; SPSS, Chicago, Illinois) was used for statistical analysis. The results were presented as the mean ± standard deviation for continuous variables with a normal distribution and as the median (interquartile range) for continuous variables with nonnormal distribution. Descriptive

statistics were expressed as proportions (percentage) for categorical variables. The Pearson χ^2 test was used when testing associations of independent categorical variables. A P value < .05 was considered statistically significant.

RESULTS

Risk Factors for Requirement of Adjunctive Embolization

Forty-two of 122 patients (34.4%) undergoing 43 of 138 procedures (31.2%) needed repeat or adjunctive embolization of hepaticoenteric anastomotic vessels at the time of ⁹⁰Y administration. An additional eight of 122 patients required adjunctive embolization for parasitized vessels but were not included in this subset analysis. The need for further embolization of hepaticoenteric communications was not related to patient age ($P = .756$); tumor cell type ($P = .522$); radioembolic product used ($P = .819$); presence of variant arterial anatomy ($P = .318$); or history of surgery ($P = .788$); transplantation ($P = .311$); chemoembolization ($P = .398$); radiofrequency ablation ($P = .745$); systemic chemotherapy ($P = .858$); antiangiogenic therapy with bevacizumab, sor-
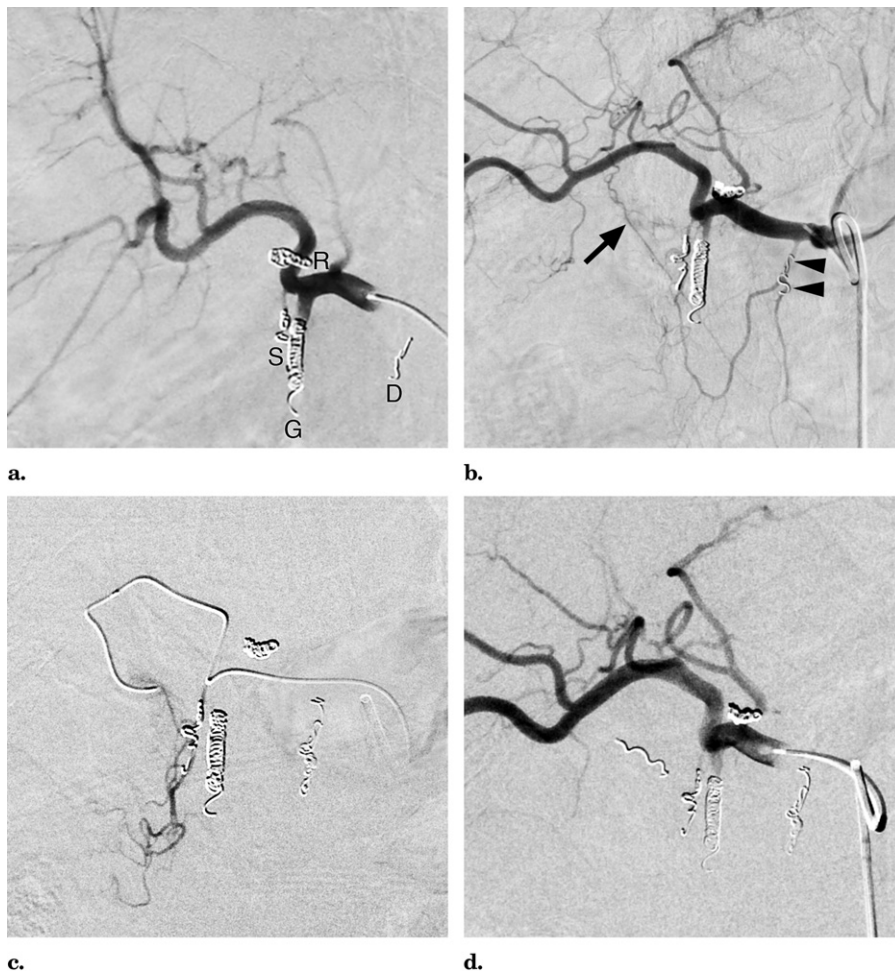
Figure 3. A 60-year-old man with metastatic colon adenocarcinoma who had undergone resection of the primary tumor and adjuvant FOLFOX and bevacizumab, underwent radioembolization for progressive bilobar hepatic metastases. **(a)** During the preparatory angiogram, the GDA (G), RGA (R), a supraduodenal artery (S), and a dorsal pancreatic artery (D) were coil embolized to stasis, resulting in satisfactory skeletonization of the hepatic artery. **(b)** At the time of radioembolic microsphere administration 14 days later, repeat hepatic arteriogram showed the appearance of a new supraduodenal artery arising from the distal right hepatic artery (arrow) as well as persistent flow through the previously placed coils in a now hypertrophied dorsal pancreatic artery (arrowheads). **(c)** The new supraduodenal artery was selected with a J-tip low profile microcatheter (Prowler 10, Cordis Neurovascular) and embolized with a 0.010-inch 2 mm x 2 cm detachable coil (Micrus). The dorsal pancreatic artery was reembolized with additional pushable coils. **(d)** Common hepatic arteriogram after reembolization confirmed successful skeletonization. This patient underwent single-session whole-liver treatment with administration into the proper hepatic artery without gastrointestinal complications.

afenib, and/or sunitinib ($P = .184$); and targeted anti–epidermal growth factor receptor therapy with cetuximab and/or panitumumab ($P = .074$). Of note, the mean and median interval between the last dose of antiangiogenic agent and the treatment angiogram were 143.2 and 82.5 days, respectively.

Women showed an insignificant trend toward requiring reembolization ($P = .058$), compared with men. This trend was not attributable to any other related risk factors. In addition, women showed a higher incidence of transcapsular invasion of the diaphragm or chest wall with parasitization of extrahepatic arteries, but parasitized arteries were excluded from our analyses.

Imaging Findings and Angiographic Evaluation of Hepatic Vasculature

The arteries that required adjunctive embolization on the day of treatment, and the vascular territories they supplied are listed in **Table 5**. The mean and median time interval between the first and second embolization procedures were 17.6 and 14.0 days (range,1–80; SD = 15.9) in those requiring repeat embolization compared with 14.7 and 13.5 (range, 1–72, SD = 10.1) in those who did not require repeat embolization ($P = .297$; **Fig 1**).

In patients in whom persistent or new hepaticoenteric anastomoses were identified, embolization of one artery was required in 28 patients (65.1%), two arteries in 12 patients (27.9%) and three arteries in three patients (7.0%) (**Table 5**). Of these, 14 arteries (23.0%) had been previously coil embolized but had either recanalized (presumably because of inadequate length or density of coil packing or had developed hypertrophied proximal branches originating from the stump, circumventing the original coils. Four of these were large GDAs with reestablished flow through previously placed coils, and four were GDAs that developed interval hypertrophy of proximal superior pancreaticoduodenal branches from the stump of the GDA. Other previously embolized arteries that showed persistent flow through coils on the treatment day were the accessory left gastric artery (LGA), RGA ($n = 2$ each), and the supraduodenal and pancreaticoduodenal arteries ($n = 1$ each).

Of the 42 patients requiring additional embolization, ^{99m}TcMAA scintigraphy identified extrahepatic perfusion in only three cases (7.1%). DSA alone was sufficient to identify 33 vessels in 22 patients (54.1% and 52.4%, respectively), and CACT alone was sufficient to identify three vessels in three patients (4.9% and 7.1%). However, a combination of both (CACT first to identify extrahepatic tissue enhancement and DSA to identify the actual vessel) was necessary to identify 25 vessels in 17 patients (41.0% and 40.5%). Ultimately, hepaticoenteric anastomoses were depicted and identified by DSA in 42 patients before repeat embolization attempts. These arteries were generally small
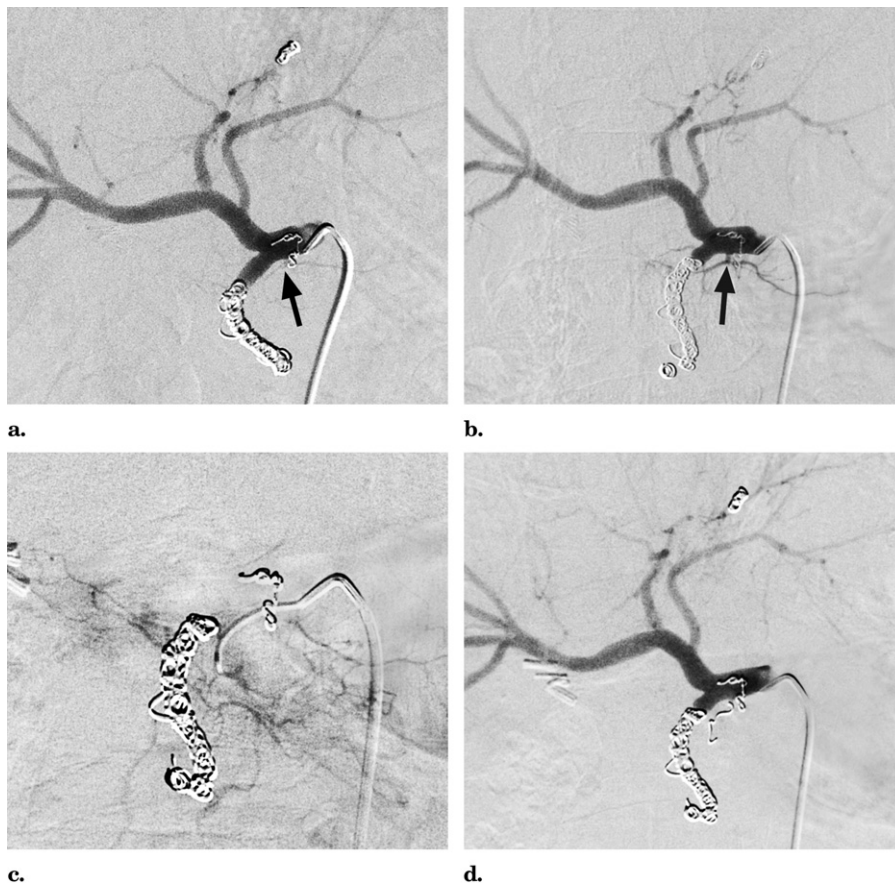
Figure 4. A 60-year-old man with a small adenocarcinoma in the tail of the pancreas presented with pain from multiple large hepatic metastases in both lobes and underwent radioembolization. **(a)** After coil embolization of the GDA, RGA, and an accessory left hepatic artery, common hepatic angiography revealed a small pancreatic artery arising from the common hepatic artery, partially obscured by the RGA coils (arrow). Attempts to catheterize this branch were unsuccessful despite using multiple different guide wires and catheters. **(b)** Before the administration of radioembolic microspheres 19 days later, a repeat hepatic angiogram showed interval hypertrophy of the branch. **(c)** The branch was successfully selected with a J-tip microcatheter (Prowler Plus, Cordis), and DSA and CACT imaging confirmed perfusion of the neck of the pancreas. **(d)** This branch was embolized successfully with two figure-of-eight coils (Target/Boston Scientific). This patient underwent single-session whole-liver treatment with administration into the proper hepatic artery without complications.

in diameter; of the 14 vessels previously embolized, five measured ≤ 2 mm (35.7%), three measured 2–4 mm (21.4%), and six measured > 4 mm (42.9 %). Of the 47 new vessels requiring embolization, 36 measured ≤ 2 mm (76.6%), 10 measured 2–4 mm (21.3%), and 1 measured > 4 mm (2.1%; **Table 6**).

Despite the small luminal diameters, 54 of 61 (88.5%) identified and targeted arteries were successfully occluded using coils, gelatin sponge (SurgiFoam, Ethicon, Somerville, New Jersey), n-tert-butyl-cyanoacrylate glue (TruFill, Cordis Neurovascular), and/or

intentional vessel occlusion by aggressive wire manipulation. Six arteries (9.8%) including three RGA and three supraduodenal arteries were managed by distal positioning of the microcatheter, five of which required splitting the dose into separate lobar or segmental doses. One falciform artery arising from the distal left hepatic artery could not be catheterized and could not be avoided by distal catheter positioning. This patient's left lobe was treated with proximal microsphere administration after placement of a bag of crushed ice on the anterior abdominal surface to vasoconstrict the

superficial body wall vessels, a technique we frequently use when chemoembolizing parasitized extrahepatic arteries.

Retrospective review of DSA and CACT images obtained during the preparatory angiogram were compared with those obtained immediately before ^{90}Y administration to determine whether the vessels were detectable on the preparatory angiogram and to help elucidate the mechanism of appearance of vessels requiring adjunctive embolization. Twelve of 61 vessels (19.7%) were not apparent on the preparatory angiogram even in retrospect and appeared de novo, likely representing interval hypertrophy of collateral vessels previously too small to detect or interval reversal of flow in vessels that previously had hepatopetal flow (**Table 7**; **Figs 2, 3**). Forty-nine vessels (80.3%) were apparent on the preparatory angiogram. In 19 of these vessels (31.1%), catheterization attempts were unsuccessful during the preparatory session (**Fig 4**), but were successful on the treatment date. For 10 vessels (16.4%), catheterization was not attempted during preparatory angiography because the luminal diameter was deemed too small to allow selection with a microcatheter; the vessels then hypertrophied to a size large enough to accept catheterization by the time of ^{90}Y administration. Ten previously embolized vessels (16.4%) showed recanalization or persistent flow through deposited coils (**Fig 3**), whereas four previously embolized vessels (6.6%) showed development or hypertrophy of a proximal branch arising from the remaining stump (**Fig 5**). Physician oversight in interpretation of the preparatory angiogram accounted for six of the vessels (9.8%) needing adjunctive embolization. The arteries that escaped detection because of human error included one falciform artery (**Fig 6**), one RGA (**Fig 7**), one accessory RGA, two cystic arteries with branches serving the duodenum, and one accessory LGA.

Treatment Complications

Of 122 patients who underwent preparatory and treatment angiography for radioembolization, six (4.9%) suffered an iatrogenic dissection of the celiac or hepatic artery. Four of these
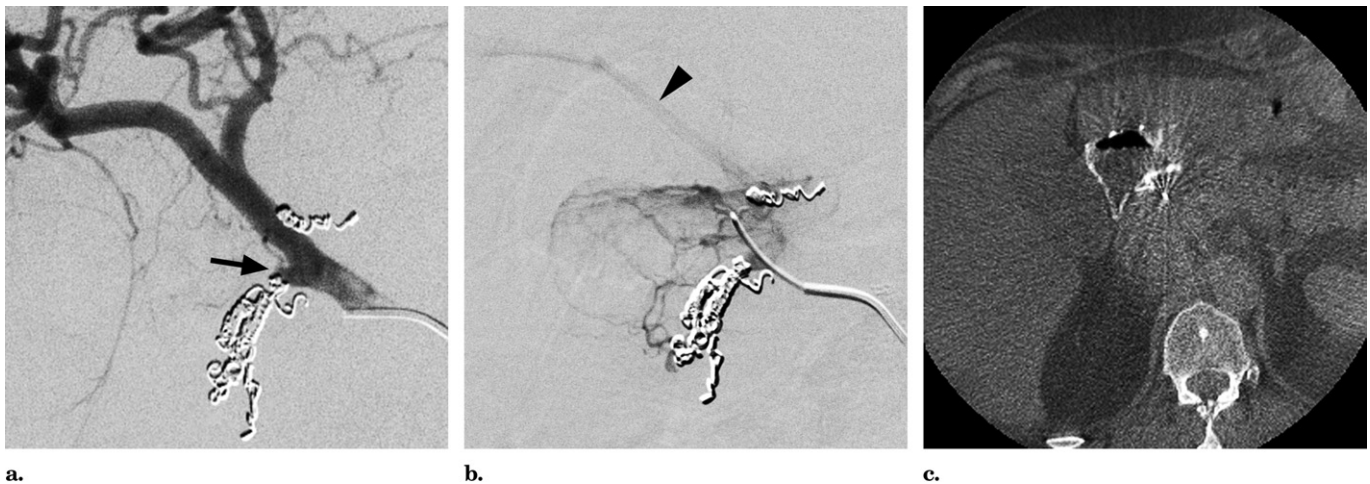
Figure 5.   A 45-year-old woman with metastatic colon adenocarcinoma and progression of bilateral hepatic metastases despite FOLFOX regimen was becoming disabled by peripheral neuropathy and elected to undergo radioembolization. After coil embolization of the RGA, GDA, and three superior pancreaticoduodenal branches of the GDA, the hepatic artery appeared to be completely skeletonized. **(a)** At the time of radioembolic microsphere administration 3 days later, a new duodenal artery was found (arrow) arising from the stump of the GDA. **(b)** Selective DSA through a microcatheter in this branch enhanced a hollow structure with venous drainage into the portal vein (arrowhead). **(c)** CACT with injection of contrast medium confirmed perfusion of the duodenal bulb. This branch was successfully coil embolized, and this patient underwent single-session whole-liver treatment with administration into the proper hepatic artery without complications.

occurred during the preparatory angiogram and embolization and two during the treatment session. Four occurred specifically during catheter manipulation for purposes of branch embolization. The injuries were caused by a 5-F catheter ($n = 4$), by a tip-deflecting microcatheter ($n = 1$; Venture; St. Jude Medical, St. Paul, Minnesota), or by a microwire ($n = 1$). Four were treated successfully by selection of the true lumen and gentle balloon dilatation, and one was treated by fenestration of the flap. Treatment was postponed in one patient and performed 6 weeks later after CT angiography confirmed healing of the dissection. Five of six patients (83.3 %) had been treated previously with bevacizumab.

Follow-up time ranged from 1 to 38 months (mean, 6.8; median, 4). Three of the 42 patients (7.1%) who underwent adjunctive embolization immediately before ^{90}Y administration had gastric or duodenal ulceration, two with biopsy-proven nontarget radioembolization. Of the 80 patients who did not require adjunctive embolization, only one had ulceration (1.3%), also biopsy proven (**Table 8**). Of the four patients in whom ulcerations developed, all underwent whole-liver treatment with resin microspheres by nonselective administration into the

proper hepatic artery. All four patients were treated successfully with prolonged courses of high-dose proton pump inhibitors and did not require surgical intervention. No patient had complications localized to the pancreas, bile ducts, gallbladder, or body wall.

DISCUSSION

Selective internal radiation therapy or radioembolization of hepatic malignancies by intraarterial infusion of microspheres containing ^{90}Y is a form of brachytherapy that has received approval by the US Food and Drug Administration and is gaining acceptance in the oncologic community (1,2,5). Clinical investigations of this therapy in different tumor types have found promising results in hepatocellular carcinoma (13) as well as in metastatic disease from colorectal cancer, neuroendocrine cancer, breast cancer, melanoma, and other tumor types (14–17). However, serious complications, such as gastrointestinal ulceration, may occur even at centers with the most experienced staff (7,18–23). Prevention of ulceration from nontarget radioembolization requires meticulous hepatic angiography and embolization (8,9). The inability to prevent reflux or administration of radioem-

bolic microspheres into the gastrointestinal tract and other extrahepatic tissue is widely acknowledged as an absolute contraindication to radioembolization (2). However, because the radioembolic material is not radiographically detectable, real-time tracking of administration is not feasible, and hemodynamic changes during ^{90}Y administration introduce additional uncertainty.

Historically, skeletonization of the hepatic artery was introduced as a surgical procedure, performed mostly in situations in which an infusion pump or port was being placed for intraarterial chemoinfusion (24). The open surgical procedure is also technically challenging, and resulted in gastrointestinal ulceration from presumed nontarget chemoinfusion in up to 24% of patients (25–27).

The known consequences of extrahepatic deposition of chemotherapeutic or radioembolic agents (including from transarterial chemoembolization) include skin and body wall necrosis, cholecystitis, pancreatitis, diaphragmatic injury, and neurological injury (7,8,28). Gastrointestinal ulceration rates after radioembolization have been reported to be as high as 29% in single-center series but average 8% in larger multicenter cohorts (18,20,22). With increased awareness, reported rates
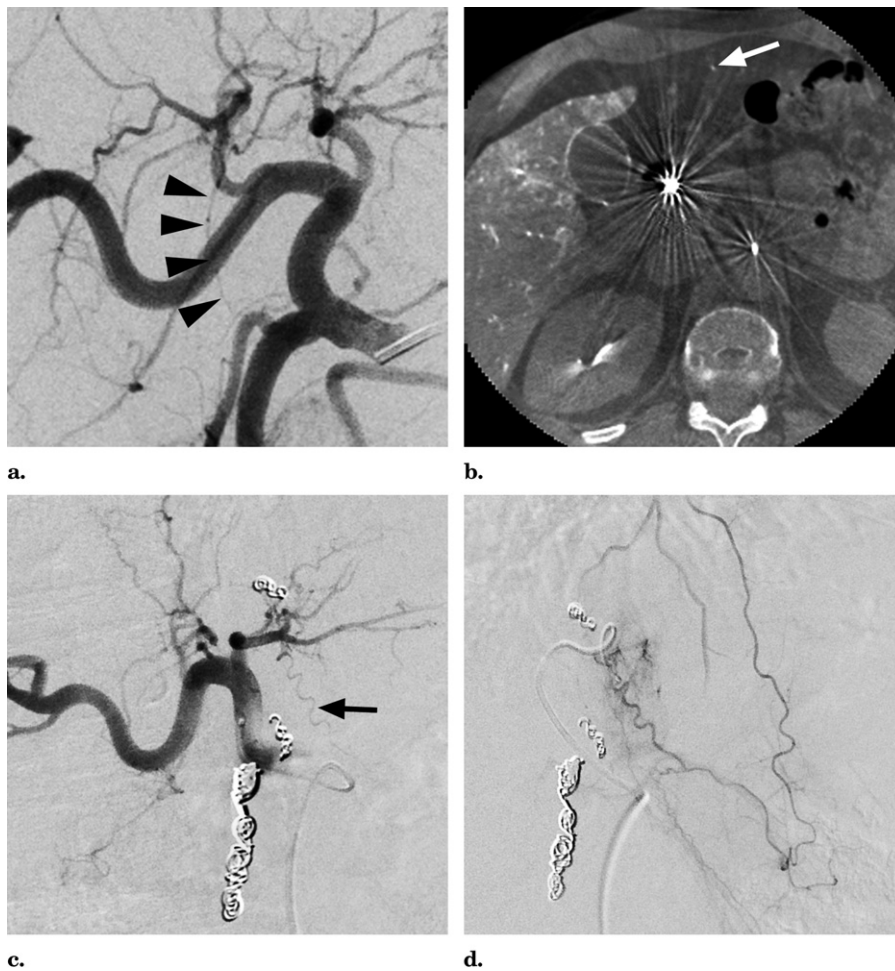
a.

b.

c.

d.

Figure 6. A 47-year-old man with metastatic colon adenocarcinoma had undergone sigmoid colectomy, hepatic wedge resection, and adjuvant FOLFOX treatment with bevacizumab but showed progressive bilobar hepatic metastases and sought radioembolization treatment. **(a)** On the initial hepatic DSA, a small falciform artery (arrowheads) was depicted but was not noticed by the operators. **(b)** After coil embolization of the GDA, RGA, and an accessory left hepatic artery, a contrast-enhanced CACT with injection in the proper hepatic artery showed enhancement of the falciform artery (arrow), which again went unrecognized. **(c)** At the time of radioembolic microsphere administration 31 days later, a right anterior oblique DSA showed the typical sine-wave appearance of the falciform artery (arrow). **(d)** Selective DSA of this artery confirmed communication with the right superior epigastric artery and anterior intercostal arteries, supplying the anterior abdominal and thoracic wall. This branch was successfully coil embolized, and this patient underwent single-session whole-liver administration from the proper hepatic artery without complications.

have mostly decreased to < 5% (7,23). Both surgical and endovascular skeletonization may be limited by the anatomic complexity of the hepatic hilum, in which many larger arteries are interconnected by a network of smaller vessels that can potentially provide collateral flow. Even after initial successful isolation of the liver, later failures may still occur. Our data show only an insignificant trend correlating longer waiting periods be-

tween preparatory and treatment procedures with a higher likelihood of formation of collateral vessels.

However, patients in whom collateral vessels develop remain at increased risk for nontarget radioembolization even after these new vessels have been embolized. This may reflect a more luxuriant hilar arterial network with greater capacity to form new collateral vessels, some of which could elude detection at the time of micro-

sphere administration. Also, formation of new collateral vessels from the hepatic bed could indicate poor communication with the superior mesenteric artery and other potential supplies of collateral perfusion. After skeletonization of the hepatic artery, collateral perfusion to the embolized territories develops in most patients through the inferior pancreaticoduodenal, left gastric, left gastroepiploic, short gastric, and transverse pancreatic arteries. If these other potential sources are congenitally absent, poorly developed, or compromised by prior therapies, these patients may continue to recruit collateral pathways preferentially from a hepatic arterial source after initial skeletonization.

All four of our patients in whom gastrointestinal ulceration developed underwent whole-liver single-session treatment with administration into the proper hepatic artery. All four were treated with resin microspheres, with which there is a greater issue of stasis and reflux. Most of the hepaticoenteric communications requiring embolization or adjunctive embolization arose from the common or proper hepatic arteries. In view of these new data, we have modified our standard method of whole-liver single-session treatment and now routinely split the dose and administer sequentially in a lobar fashion with two successive microcatheterizations. This modification may also reduce the risk of injury to hepatic vessels that can result from challenging embolization attempts, particularly in the patient population with fragile vessels from prior chemotherapeutic and antiangiogenic therapies. Even with sequential lobar administrations, special attention must be paid to detect distal hepaticoenteric communications including falciform, accessory phrenic, and accessory left gastric arteries branching from the distal left hepatic artery and supraduodenal and ductal arteries branching from the distal right hepatic artery.

Recent advances in angiographic imaging technology have facilitated detection of small hepaticoenteric anastomoses. Modern flat-panel detector DSA uses a pixel size of about 150 μm, allowing resolution of 3.25 line pairs per millimeter and depiction of submillimeter vessels. In addition, the availability of CACT imaging using
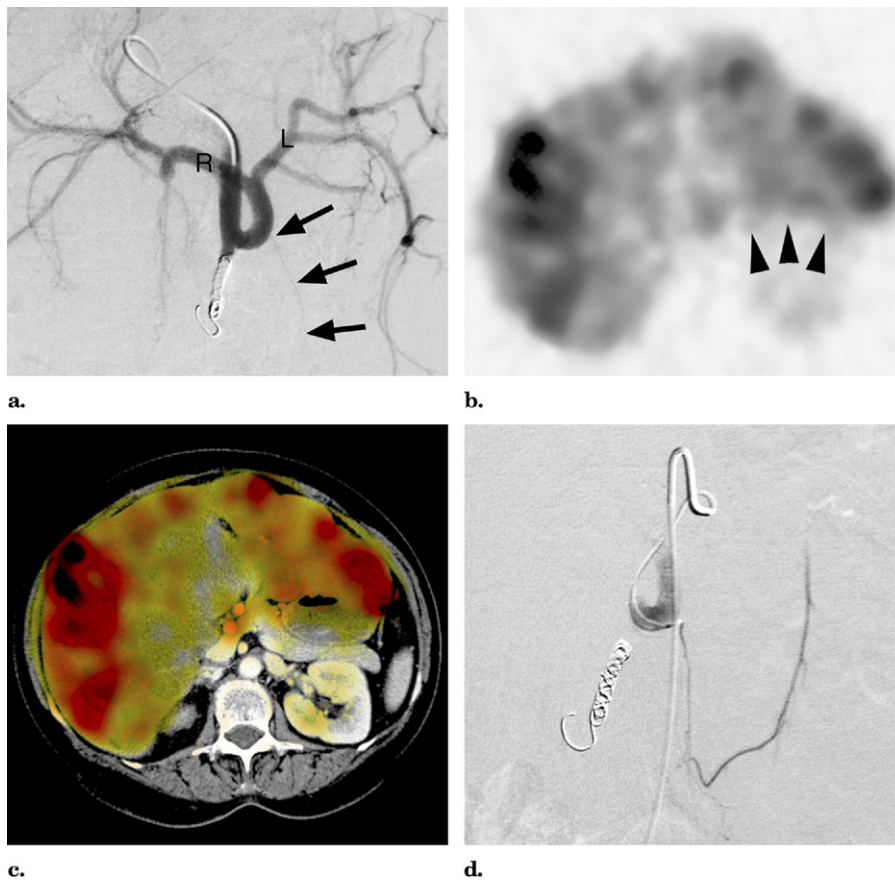
a.

b.

c.

d.

Table 8
Gastrointestinal Ulcerative Complications

	n	%
Patients requiring adjunctive embolization	3/42	7.1
Patients not requiring adjunctive embolization	1/80	1.3
Total	4/122	3.3

Note.—$\chi^2 = 6.536$; $P = .038$.

Figure 7. A 61-year-old woman with retroperitoneal leiomyosarcoma metastatic to bone, lungs, and liver had undergone surgical resection of the primary tumor with adjuvant radiotherapy, multiple regimens of systemic chemotherapy including ifosfamide, doxorubicin, dacarbazine, temozolomide, gemcitabine, docetaxel, and sorafenib, and radiotherapy to osseous metastases. The hepatic metastases had progressed to the point of enlarging the liver to a volume of approximately 4 liters. **(a)** Common hepatic artery DSA after embolization of the GDA showed leftward deviation of the proper hepatic artery caused by massive enlargement of the liver, and both the right (R) and left (L) hepatic arteries originating from the left upper quadrant. The RGA originated from the proper hepatic artery to the left of the GDA (arrows) but was not identified by the operators during the procedure because of the distortion and displacement of vessels. **(b)** Deposition of ^{99m}TcMAA in the anterior lesser curve of the stomach (arrowheads) was revealed by SPECT scintigraphy, but required careful registration onto a previous CT scan to confirm extrahepatic location **(c).** This was one of only three patients in whom scintigraphy identified extrahepatic deposition. **(d)** The artery was identified 15 days later at the time of radioembolic microsphere administration and was selected and coil embolized. This patient also underwent single-session whole-liver administration from the proper hepatic artery without gastrointestinal complications.

the same equipment and without moving the patient allows high-sensitivity detection of enhanced tissue and three-dimensional angiography, greatly improving the ability to identify and to locate these anastomoses (11). Detection of vessels does not guarantee technical success in cannulation and embolization of these vessels, but knowledge of these communications even without successful embolization may influence treatment planning and

may prompt more distal catheter positioning for microsphere administration. Currently, no data show whether detection of and embolization or avoidance of vessels detectable only by high-sensitivity equipment makes a significant impact on the rate of nontarget radioembolization, but our overall 3.3% rate of ulcerative complications compares favorably with those in the literature. ^{99m}TcMAA scintigraphy, although very useful for cal-

culation of lung dose, is of very limited utility for identification of extrahepatic perfusion, with a sensitivity of only 7.1% in our series. Its sensitivity is limited by spatial resolution and also by the fact that it is performed at the time of initial skeletonization before many collateral vessels have had time to appear. Although we did not perform real-time SPECT-CT, superimposition of SPECT images on prior CT images helped to demarcate intra- and extrahepatic ^{99m}TcMAA deposition in some patients but with resolution clearly inferior to that of DSA combined with CACT.

Yttrium-90 radioembolization therapy is a complex procedure that requires meticulous angiographic technique for optimal safety and success. Our data showed that despite initial successful skeletonization of the hepatic artery, new hepaticoenteric pathways were frequently discovered at the time of ^{90}Y administration. Contrast-enhanced CACT was necessary in detection of half of these vessels. The collateral vessels may be managed by additional embolization or by catheter repositioning to avoid nontarget radioembolization. However, patients in whom new collateral channels developed appeared to have a persistently increased risk of gastrointestinal ulceration after radioembolization, even if the newly appearing channels were embolized successfully.

References
1. Salem R, Thurston KG. Radioembolization with yttrium-90 microspheres: a state-of-the-art brachytherapy treatment for primary and secondary liver malignancies: part 3: comprehensive literature review and future direction. J Vasc Interv Radiol 2006; 17:1571–1593.
2. Kennedy A, Nag S, Salem R, et al. Recommendations for radioemboliza-

tion of hepatic malignancies using yttrium-90 microsphere brachytherapy: a consensus panel report from the radioembolization brachytherapy oncology consortium. Int J Radiat Oncol Biol Phys 2007; 68:13–23.

3. Ariel IM. Treatment of inoperable primary pancreatic and liver cancer by the intra-arterial administration of radioactive isotopes (Y90 radiating microspheres). Ann Surg 1965; 162:267–278.

4. Simon N, Silverstone SM, Roach LC, et al. Intra-arterial irradiation of tumors, a safe procedure. Am J Roentgenol Radium Ther Nucl Med 1971; 112:732–739.

5. Salem R, Thurston KG. Radioembolization with 90yttrium microspheres: a state-of-the-art brachytherapy treatment for primary and secondary liver malignancies. Part 2: special topics. J Vasc Interv Radiol 2006; 17:1425–1439.

6. Murthy R, Nunez R, Szklaruk J, et al. Yttrium-90 microsphere therapy for hepatic malignancy: devices, indications, technical considerations, and potential complications. Radiographics 2005; 25 Suppl 1:S41–55.

7. Riaz A, Lewandowski RJ, Kulik LM, et al. Complications following radioembolization with yttrium-90 microspheres: a comprehensive literature review. J Vasc Interv Radiol 2009; 20:1121–1130; quiz 1131.

8. Liu DM, Salem R, Bui JT, et al. Angiographic considerations in patients undergoing liver-directed therapy. J Vasc Interv Radiol 2005; 16:911–935.

9. Lewandowski RJ, Sato KT, Atassi B, et al. Radioembolization with 90Y microspheres: angiographic and technical considerations. Cardiovasc Intervent Radiol 2007; 30:571–592.

10. Hamami ME, Poeppel TD, Muller S, et al. SPECT/CT with 99mTc-MAA in radioembolization with 90Y microspheres in patients with hepatocellular cancer. J Nucl Med 2009; 50:688–692.

11. Louie JD, Kothary N, Kuo WT, et al. Incorporating cone-beam CT into the treatment planning for yttrium-90 radioembolization. J Vasc Interv Radiol 2009; 20:606–613.

12. Sze DY LJ, Iagaru A, Abdelmaksoud M, Goris ML. Survival after radioembolization is predicted by dose distribution scintigraphy fusion imaging. J Vasc Interv Radiol 2010; 21(Suppl 2):S10.

13. Salem R, Lewandowski RJ, Mulcahy MF, et al. Radioembolization for hepatocellular carcinoma using Yttrium-90 microspheres: a comprehensive report of long-term outcomes. Gastroenterology 2010; 138:52–64.

14. Gray B, Van Hazel G, Hope M, et al. Randomised trial of SIR-Spheres plus chemotherapy vs. chemotherapy alone for treating patients with liver metastases from primary large bowel cancer. Ann Oncol 2001; 12:1711–1720.

15. Geschwind JF, Salem R, Carr BI, et al. Yttrium-90 microspheres for the treatment of hepatocellular carcinoma. Gastroenterology 2004; 127:S194–205.

16. Sato KT, Lewandowski RJ, Mulcahy MF, et al. Unresectable chemorefractory liver metastases: radioembolization with 90Y microspheres—safety, efficacy, and survival. Radiology 2008; 247:507–515.

17. Vente MA, Wondergem M, van der Tweel I, et al. Yttrium-90 microsphere radioembolization for the treatment of liver malignancies: a structured meta-analysis. Eur Radiol 2009; 19:951–959.

18. Murthy R, Brown DB, Salem R, et al. Gastrointestinal complications associated with hepatic arterial Yttrium-90 microsphere therapy. J Vasc Interv Radiol 2007; 18:553–561; quiz 562.

19. Salem R, Lewandowski RJ, Sato KT, et al. Technical aspects of radioembolization with 90Y microspheres. Tech Vasc Interv Radiol 2007; 10:12–29.

20. Carretero C, Munoz-Navas M, Betes M, et al. Gastroduodenal injury after ra-

dioembolization of hepatic tumors. Am J Gastroenterol 2007; 102:1216–1220.

21. Konda A, Savin MA, Cappell MS, Duffy MC. Radiation microsphere-induced GI ulcers after selective internal radiation therapy for hepatic tumors: an underrecognized clinical entity. Gastrointest Endosc 2009; 70:561–567.

22. Neff R, Abdel-Misih R, Khatri J, et al. The toxicity of liver directed yttrium-90 microspheres in primary and metastatic liver tumors. Cancer Invest 2008; 26:173–177.

23. Naymagon S, Warner RR, Patel K, et al. Gastroduodenal ulceration associated with radioembolization for the treatment of hepatic tumors: an institutional experience and review of the literature. Dig Dis Sci 2010; Mar 3. Epub ahead of print.

24. Cohen AD, Kemeny NE. An update on hepatic arterial infusion chemotherapy for colorectal cancer. Oncologist 2003; 8:553–566.

25. Ikeda O, Tamura Y, Nakasone Y, et al. Evaluation of extrahepatic perfusion of anticancer drugs in the right gastric arterial region on fused images using combined CT/SPECT: is extrahepatic perfusion predictive of gastric toxicity? Cardiovasc Intervent Radiol 2007; 30:392–397.

26. Proietti S, De Baere T, Bessoud B, et al. Interventional management of gastroduodenal lesions complicating intra-arterial hepatic chemotherapy. Eur Radiol 2007; 17:2160–2165.

27. Ravizza D, Fazio N, Fiori G, et al. Iatrogenic gastroduodenal ulcers during hepatic intra-arterial chemotherapy. Hepatogastroenterology 2003; 50:49–53.

28. Leong QM, Lai HK, Lo RG, et al. Radiation dermatitis following radioembolization for hepatocellular carcinoma: a case for prophylactic embolization of a patent falciform artery. J Vasc Interv Radiol 2009; 20:833–836.